Radiation damage of protein crystals at cryogenic temperatures between 40 K and 150 K

Tsu-Yi Teng* and Keith Moffat

Department of Biochemistry and Molecular Biology, The University of Chicago, Chicago, IL 60637, USA. E-mail: t-teng@uchicago.edu

X-ray radiation damage of lysozyme single crystals by an intense monochromatic beam from the Advanced Photon Source is studied at cryogenic temperatures between 40 K and 150 K. The results confirm that primary radiation damage is both linearly dependent on the X-ray dose and independent of temperature. The upper limit for the primary radiation damage observed in our previous study [Teng & Moffat (2000), *J. Synchrotron Rad*. **7**, 313–317] holds over the wider temperature range of this study. The X-ray diffraction quality of the data acquired at 40 K is superior to those at 100 K, apparently due to temperature dependence of secondary and tertiary radiation damage and to reduced thermal motion.

Keywords: protein crystals; radiation damage; monochromatic radiation.

1. Introduction

The study of X-ray radiation damage of protein crystals has drawn much attention in recent years. The reason is simple: the apparently indefinite life of frozen protein crystals when exposed to an X-ray beam from second-generation synchrotron sources is greatly reduced when such crystals are exposed to the more intense beams from third-generation sources (Garman, 1999; Walsh *et al.*, 1999).

In order to fully utilize the intense X-ray beams now available, quantitative understanding of X-ray-induced radiation damage becomes an urgent task. The interaction between X-ray photons and molecules in the crystal lattice causes two types of damage, physical and chemical (Teng & Moffat, 2000; see also Arndt, 1984; Helliwell, 1992). For a monochromatic oscillation experiment, chemical damage is the major concern. A better understanding of the factors that give rise to chemical damage through the production and diffusion of radicals in protein crystals and in frozen solution is essential. Five studies on X-ray radiation damage from third-generation synchrotron sources were published in the year 2000 alone (Burmeister, 2000; Glaeser *et al.*, 2000; Ravelli & McSweeney, 2000; Teng & Moffat, 2000; Weik *et al.*, 2000), in which a wide variety of protein crystals were investigated at different beamlines. These studies took two different yet complementary approaches. The first approach emphasizes the study of diffraction data in reciprocal space; the second emphasizes structural damage in real space. Our study (Teng & Moffat, 2000) and that of Glaeser *et al.* (2000) clearly belong to the first approach; those of Burmeister (2000), Ravelli & McSweeney (2000) and Weik *et al.* (2000) belong mostly to the second. In reciprocal space, the reduction in diffraction quality caused by X-ray radiation damage is evident in the decay of diffraction intensities and in the increase of unit-cell volume, overall *B*-factor and merged *R*-factor. In real space, structural refinement shows that damage is more severe at certain chemical sites, for example rupture of disulfide bonds, decarboxylation of aspartates and loss of tyrosine hydroxyl groups. Not all sites of a given chemical type are equally sensitive to radiation damage. Based on these observations, the routes by which mobile electrons produce specific chemical damage were proposed (Ravelli & McSweeney, 2000; Weik *et al.*, 2000).

Our previous study (Teng & Moffat, 2000) made a clear differentiation between primary and secondary radiation damage. We observed that the decay of diffraction quality is linearly dependent on X-ray dose over a region where primary damage dominates up to an apparent threshold of 1×10^7 Gy, above which secondary and tertiary damage become apparent. By considering the scattering power of protein crystals, we proposed a practical limit for macromolecular crystallography. Our results are in good agreement with those of other studies. Table 1 lists the upper limit for X-ray radiation damage and the estimated lifetime of a 100 μm protein crystal, suggested by three of the studies.

We now ask: how do radiation damage and data quality depend on temperature, in the cryogenic range? Is primary radiation damage indeed independent of temperature, as expected? Do other components of damage depend on temperature?

2. Materials and methods

Crystal preparation, flash cooling of crystals, synchrotron beamline, experimental set-up and data reduction were all as previously described (Teng & Moffat, 2000).

A total of five hen egg-white lysozyme single crystals were studied at three temperatures, 40 K, 100 K and 150 K. Temperatures of 40 K and 100 K were provided by a helium gas stream from the liquid-helium/liquid-nitrogen cryostat (Teng *et al.*, 1994); temperatures of 100 K and 150 K were provided by a nitrogen gas stream from a commercial crystal cooler (Molecular Structure Corporation, Woodland, TX, USA). Two crystals (Table 2, crystals 2 and 4) were used to record data continuously but the temperature alternated between 40 K and 100 K (or 150 K and 100 K) from one data set to the next. Two other crystals (Table 2, crystals 1 and 5) were maintained at a constant temperature of 40 K or 150 K, but irradiated by a long X-ray exposure between data sets. Data on crystal 3 at 100 K were those obtained in our previous study (Teng & Moffat, 2000). Table 2 summarizes the total dose absorbed at the completion of each data set and the temperature at which the data set was taken, for each crystal. Compared with the previous study, the dose absorbed by each crystal was higher and the extent of radiation damage at the end of each experiment was larger.

3. Results and discussion

In our previous study (Teng & Moffat, 2000), a striking quantitative feature was observed, that the effect of radiation damage on several

Table 1
Comparison of the upper limit for X-ray radiation damage and the lifetime of a 100 μm protein crystal (Teng & Moffat, 2000; Glaeser *et al.*, 2000; Burmeister, 2000).

	Teng & Moffat	Glaeser *et al.*	Burmeister
Diffraction power of crystal used	3.3×10^{12}	1.2×10^{12}	2.4×10^{12}
Suggested limits in:			
Dose (Gy)	1×10^7	–	3×10^7
Dose (photons mm^{-2})	2×10^{16}	$\sim 10^{16}$	4×10^{16}
Number of unit cells needed for 100 images	3×10^{11}	$\sim 10^{11}$	–
Minimum crystal size needed for 100 images (μm)	35	37	~30
Minimum crystal size needed for one image (μm)	8	7.4	–
Estimated crystal lifetime (10^3 s)	11	135	3.6

Table 2
Summary of data sets taken from crystals used in the study.

Data set	1	2	3	4	5	6	7	8	9	10	11	12	13	14	15
Crystal 1															
Temperature (K)	40	40	40	40	40	40	40	40	40	40					
Dose (10^7 Gy)	0.24	0.72	1.20	1.69	2.17	2.64	3.14	3.62	4.11	4.60					
Crystal 2															
Temperature (K)	40	100	40	100	40	100	40	100	40	100	40	100	40	100	
Dose (10^7 Gy)	0.24	0.48	0.72	0.96	1.19	1.42	1.64	1.85	2.03	2.20	2.38	2.56	2.72	2.89	
Crystal 3															
Temperature (K)	100	100	100	100	100	100	100	100							
Dose (10^7 Gy)	0.12	0.34	0.55	0.76	0.96	1.16	1.36	1.55							
Crystal 4															
Temperature (K)	150	100	150	100	150	100	150	100	150	100	150	100	150	100	150
Dose (10^7 Gy)	0.19	0.38	0.54	0.70	0.85	1.00	1.15	1.29	1.43	1.56	1.76	1.94	2.12	2.30	2.46
Crystal 5															
Temperature (K)	150	150	150	150	150	150	150	150							
Dose (10^7 Gy)	0.18	0.52	0.84	1.15	1.45	1.73	2.01	2.27							

parameters characteristic of the diffraction data quality was linearly dependent on the absorbed dose, up to a threshold value of approximately 1×10^7 Gy. We interpreted the threshold as the upper limit of primary radiation damage. At higher values of absorbed dose, damage exceeds that predicted from the simple linear model: secondary and perhaps tertiary radiation damage effects are becoming significant. Does this conclusion hold for other temperatures in the cryogenic temperature region?

Fig. 1 shows the decay of total intensity of X-ray diffraction as a function of X-ray energy absorbed. The total intensity is a summation of intensities of all diffraction spots observed in the data set and is presented on a relative scale, *i.e.* as a fraction of the total intensity of the first data set of the crystal. A total of 55 data sets are plotted (Fig. 1). Clearly, the trend of intensity decay is identical at all three temperatures.

A simple polynomial curve fitting of all data points (solid line), or of data points at each temperature separately, results in the same initial slope of around $-(5 \pm 0.5) \times 10^{-8}$ Gy^{-1}. That is, the total diffraction intensity diminishes to half the value from a virgin crystal after absorbing an X-ray energy of 1×10^7 Gy. The dotted line represents a linear fit over the region of low X-ray dose, and clearly shows the deviation from the linear fit starts around 1×10^7 Gy.

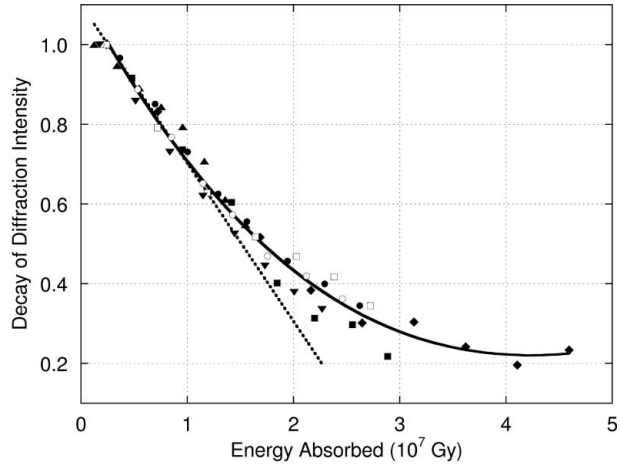

Figure 1
Intensity decay of X-ray damaged crystal. Total intensity I_T is calculated by summing all diffraction intensities I_H, thus $I_T = \sum I_H$, and then normalized by the first data set, I_{Ti}/I_1, where $i = 1, 2, \ldots$ is the data-set number of the crystal. Crystal 1 at 40 K (♦); crystal 2 at 40 K (□); crystal 2 at 100 K (■); crystal 3 at 100 K (▲); crystal 4 at 100 K (●); crystal 4 at 150 K (○); crystal 5 at 150 K (▼).

Primary radiation damage is by definition linearly dependent on the absorbed dose, and we assumed previously (Teng & Moffat, 2000) that the linear fit region arises from primary radiation damage. Our new results confirm that the upper limit for primary radiation damage observed in the previous study (Teng & Moffat, 2000) holds for all temperatures in the study. Primary radiation damage is independent of temperature in the range from 40 K to 150 K.

Burmeister fitted his data (in which five data points covered a total X-ray dose of 3.9×10^7 Gy) with an exponential function [see Fig. 2(*a*) of Burmeister (2000)], and derived an exponent of -3.3×10^{-8} Gy^{-1}. If we similarly fit our data with an exponential, it results in an exponent of $-(3.9 \pm 1.8) \times 10^{-8}$ Gy^{-1}. Thus, both studies agree beautifully. At lower X-ray doses, this exponential fit reduces to a linear fit with a slope of -4×10^{-8} Gy^{-1}, a value slightly smaller than that derived from a cubic fit above. We favor the polynomial fit, because its deviations are smaller between temperatures. In the low-dose region, both fits express the primary radiation damage well; at higher doses, we interpret our results to indicate the onset of secondary effects. However, both fits are purely mathematical since there is no simple model for describing the radiation-damage mechanism.

For all data sets, the unit-cell volume and the overall *B*-factor increase with absorbed dose at all temperatures studied (data not shown). The variation in *B*-factor from crystal to crystal is quite large, with initial values from 11.2 to 13.9 Å^2, for 100 K data. However, the *B*-factors for crystal 2 (Fig. 2) do not depend strongly on temperature. It appears that, at least for this crystal, the *B*-factor arises largely from temperature-independent, static disorder rather than from temperature-dependent, dynamic disorder (see Frauenfelder *et al.*, 1979; Hartmann *et al.*, 1982; Parak *et al.*, 1987; Tilton *et al.*, 1992). Nevertheless, data quality does appear to depend on temperature. For this crystal, Table 3 lists data-reduction statistics and Fig. 3 shows the number of reflections with $I/\sigma(I) \geq 3$, both overall and in the highest-resolution shell from 1.66 to 1.60 Å, as a function of energy absorbed. Evidently, *R*-factors, completeness and number of reflections are all superior at 40 K by comparison with 100 K. Closer examination of these data shows that the curves at 40 K and 100 K only deviate at values of the absorbed dose greater than 1 to 1.5×10^7 Gy (after completion of data set 6, Table 3). That is, the temperature dependence of diffraction quality only becomes evident at high values of the energy absorbed. Radiation damage may therefore be separated into two components: (i) temperature-independent primary radiation damage, evident at lower absorbed energies up to the threshold, and (ii) temperature-dependent secondary and tertiary radiation damage, evident only at higher absorbed energies above the threshold.

Table 3
Diffraction data reduction statistics for crystal 2.

Overall: reflections from 100 to 160 Å. Last shell: reflections from 166 to 160 Å. Merged *R*-factor, $R_{\rm merge} = \sum [{\rm ABS}(I - \langle I \rangle)]/\sum(I)$. Every data set contains 100 images except the last, which yielded only 68 usable images.

Data set	1	2	3	4	5	6	7	8	9	10	11	12	13	14
Total measurement	231035	231519	231161	233489	233347	232173	231986	232910	234113	235541	235264	236133	235633	154691
Unique reflections	15014	15110	15047	15182	15157	15210	15154	15209	15124	15218	15218	15279	15219	15304
Completeness														
Last shell	0.997	0.990	0.990	0.995	0.993	0.968	0.924	0.547	0.690	0.210	0.467	0.147	0.233	0.001
Overall	0.993	0.990	0.992	0.993	0.994	0.990	0.986	0.935	0.957	0.843	0.921	0.828	0.851	0.438
$R_{\rm merge}$														
Last shell	0.111	0.125	0.143	0.174	0.203	0.240	0.262	0.361	0.304	0.367	0.332	0.702	0.424	–
Overall	0.033	0.039	0.034	0.036	0.038	0.039	0.041	0.044	0.044	0.051	0.046	0.054	0.049	0.270
$\langle I \rangle / \langle \sigma(I) \rangle$														
Last shell	20.3	17.0	15.3	12.4	9.83	7.02	5.33	2.65	3.34	1.53	2.54	1.20	1.75	–
Overall	36.2	35.2	35.7	35.1	34.2	34,0	33.0	30.8	31.7	28.3	30.4	28.2	31.3	5.94

Data sets acquired with crystal 4 show the same tendency, but the differences between those taken at 100 K and those at 150 K are smaller (not shown).

Hanson *et al.* (1999), in an initial study using laboratory X-ray sources, reported that diffraction data from sperm-whale myoglobin crystals collected in helium gas streams at <33 K and nitrogen at ∼100 K showed a 23% lower overall *B*-factor for helium data. They also showed that the C-terminus of refined myoglobin structures was better ordered with lower atomic *B*-factors for the helium data than nitrogen. They further extended their studies by synchrotron data (Hanson *et al.*, 2000). Their comparisons were, however, based on different crystals, different X-ray sources (sealed tube *versus* rotating anode) and detectors (CCD *versus* image plate), and yielded data sets with different resolution and completeness.

Our experimental strategy, in which one crystal was cycled between two temperatures, is intended to isolate the effects of temperature and to minimize systematic errors that arise from, for example, crystal-to-crystal variation, or the use of different cryogens or experimental protocols, at different temperatures. For example, use of helium as a cryogen may result in lower background scattering and hence data that are improved over those obtained with nitrogen as a cryogen, even in the absence of temperature-dependent effects. Our comparison used the same crystal with the same X-ray source, detector and oscillation geometry and, thus, minimized systematic errors arising from variation in these parameters. We confirm that the data are better at 40 K than 100 K, but only after much higher energies have been absorbed.

In conclusion, primary X-ray damage of protein crystals is a physical process which depends on X-ray dose, photon energy and atomic absorption coefficient, but is independent of temperature. However, secondary and tertiary radiation damage depends on the nature of the chemical structure of the molecule and is temperature-dependent. Use of a helium cryostat for static data collection will only offer advantages if crystals are to be irradiated beyond the primary radiation damage limit, or if the crystal has a large component of temperature-dependent dynamic disorder.

TYT thanks Vukica Srajer for many discussions and Reinhard Pahl for help in experiment set-up. We thank all BioCARS staff for their excellent support. Use of the Advanced Photon Source was supported by the US Department of Energy, Basic Energy Sciences, Office of Science, under Contract No. W-31-109-Eng-38. Use of the BioCARS Sector 14 was supported by the National Institutes of Health, National Center for Research Resources, under grant number RR07707.

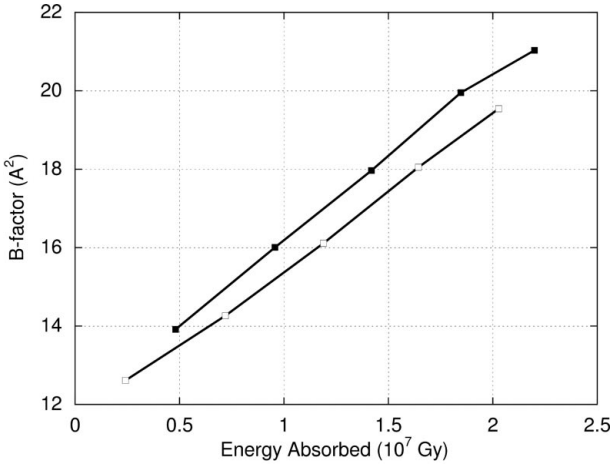

Figure 2
Comparison of the *B*-factor for crystal 2 between 40 K and 100 K, as a function of absorbed dose. Overall *B*-factors are obtained from Wilson plots. 40 K data (□); 100 K data (■). Only ten *B*-factors from a total of 14 data sets are plotted; data sets 11–14 did not yield accurate *B*-factors due to the lack of high-resolution data arising from large radiation damage.

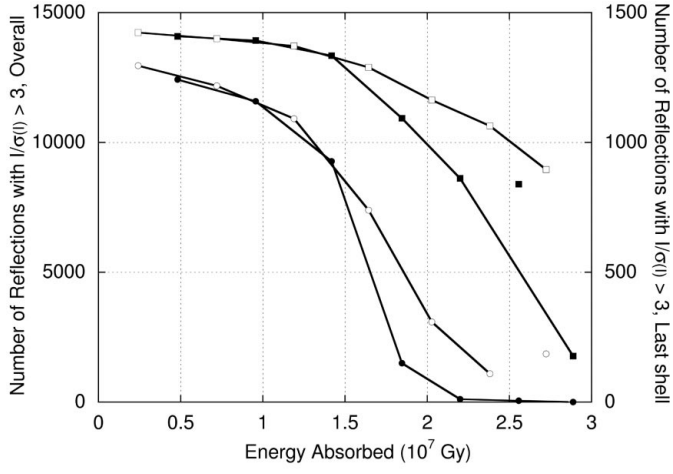

Figure 3
Decay of the number of reflections with $I/\sigma(I) \geq 3$, both overall (100–1.60 Å) and in the last shell (1.66–1.60 Å), as a function of absorbed dose and temperature for crystal 2. 40 K overall data (□); 100 K overall data (■); 40 K last-shell data (○); 100 K last-shell data (●).

References

Arndt, U. W. (1984). *J. Appl. Cryst.* **17**, 118–119.
Burmeister, W. P. (2000). *Acta Cryst.* D**56**, 328–341.
Frauenfelder, H., Petsko, G. A. & Tsernoglou, D. (1979). *Nature (London)*, **280**, 558–563.
Garman, E. F. (1999). *Acta Cryst.* D**55**, 1641–1653.
Glaeser, R., Facciotti, M., Walian, P., Rouhani, S., Holton, J., MacDowell, A., Celestre, R., Cambie, D. & Padmore, H. (2000). *Biophys. J.* **78**, 3178–3185.
Hanson, B. L., Harp, J. M., Kirschbaum, K., Parrish, D. A., Timm, D. E., Howard, A., Pinkerton, A. A. & Bunick, G. J. (2000). ACA Abstract W0102, St Paul, USA.
Hanson, B. L., Martin, A., Harp, J. M., Parrish, D. A., Bunick, C. G., Kirschbaum, K., Pinkerton, A. A. & Bunick, G. J. (1999). *J. Appl. Cryst.* **32**, 814–820.
Hartmann, H., Parak, F., Steigemann, W., Petsko, G. A., Ringe, P. D. & Frauenfelder, H. (1982). *Proc. Natl Acad. Sci. USA*, **79**, 4967–4971.
Helliwell, J. R. (1992). *Macromolecular Crystallography with Synchrotron Radiation.* Cambridge University Press.
Parak, F., Hartmann, H., Aumann, K. D., Reuscher, H., Rennekamp, G., Bartunik, H. & Steigemann, W. (1987). *Eur. Biophys. J.* **15**, 237–249.
Ravelli, R. B. G. & McSweeney, S. M. (2000). *Structure*, **8**, 315–328.
Teng, T.-Y. & Moffat, K. (2000). *J. Synchrotron Rad.* **7**, 313–317.
Teng, T.-Y., Schildkamp, W., Dolmer, P. & Moffat, K. (1994). *J. Appl. Cryst.* **27**, 133–139.
Tilton, R. F. Jr, Dewan, J. C. & Petsko, G. A. (1992). *Biochemistry*, **31**, 2469–2481.
Walsh, M. A., Dementieva, I., Evans, G., Sanishvili, R. & Joachimiak, A. (1999). *Acta Cryst.* D**55**, 1168–1173.
Weik, M., Ravelli, R. B. G., Kryger, G., McSweeney, S., Raves, M. L., Harel, M., Gros, P., Silman, I., Kroon, J. & Sussman, J. (2000). *Proc. Natl Acad. Sci. USA*, **97**, 623–628.

Received 4 December 2001 • Accepted 10 May 2002